



Texas State University



Fermi National Accelerator Laboratory

LArIAT – Neutrino Division

Aerogel Beam Line Cherenkov Detector for the LArIAT Experiment



Brandon Soubasis

Advisor: Jennifer Raaf, Karol Lang, Will Flanagan

SIST Intern, Summer 2015

Abstract:

The Liquid Argon In A Test beam (LArIAT) experiment at the Fermilab Test Beam Facility (FTBF) aims to calibrate and characterize liquid argon time projection chambers with a beam of charged particles. This will allow for critical measurements of interest to all current and proposed liquid argon detectors. Our group has designed and constructed prototypes of an aerogel Cherenkov detector to be placed along the beam line. This detector will allow us to separate incoming muons and pions in the momentum range of most interest to the LArIAT experiment.

Table of Contents

Abstract.....	1
Introduction.....	3
LArIAT.....	3
Particle Identification.....	3
Materials and Methods.....	5
Results and Future Work.....	7
Acknowledgments.....	8

Introduction

Neutrinos rarely interact with other particles, and don't leave a track as they enter a detector. LArTPCs are ideal detectors for precision neutrino physics. The Fermilab Test Beam Facility (FTBF) is the ideal place to do these studies, providing beams of not only a range of known energies, but also a selection of different particle types. A test beam also provides a controlled environment in which to tune simulations and to develop tools for particle identification (PID), calorimetry, and event reconstruction without relying solely on simulation. Fermilab has built two LArTPC for neutrino experiments. LArIAT will be a crucial input to these experiments.

LArIAT

The Liquid Argon In A Test beam (LArIAT) experiment at the Fermilab Test Beam Facility (FTBF) is a smaller version of MicroBooNe with three quarters of a ton of liquid argon instead of MicroBooNe's 170 ton which aims to calibrate and characterize liquid argon time projection chambers with beam of charged particles. This will allow for critical measurements of interest to all current and proposed liquid argon detectors.

I was able to construct a Cherenkov radiation detector to be used in the LArIAT (Liquid Argon In A Test-beam) experiment at FNAL. Using aerogel tiles within the detector will enable me to distinguish particles in the detector for the LArIAT experiment from the Cherenkov light into the photomultiplier tubes.

Particle Identification

Muons and pions interact electromagnetically, leading to a steady loss of energy through dE/dx ionization effects as they move through material. Muons are typically identified by their ability to penetrate deeply into matter. In most experiments, muon chambers consist of thick layers of steel alternated with scintillator placed outside the tracking chambers and calorimeters.

Muons do not have strong interactions and penetrate deeply into absorbers. However, pions are hadrons and behave similarly in tracking chambers and calorimeters. Time of flight information can distinguish particles in certain velocity regions. Where the velocity of a particle

$$v = \frac{p}{E} = \frac{p}{\sqrt{p^2+m^2}} = \left(1 + \frac{m^2}{p^2}\right)^{-1/2}, \text{ in units of } c. \text{ The time it takes for them to move between two}$$

positions a distance d apart is $t = \frac{d}{v} = \frac{d}{c} \left(1 + \frac{m^2}{p^2}\right)^{1/2}$, but time of flight can be difficult since

muons and pions masses only differ by 30%.

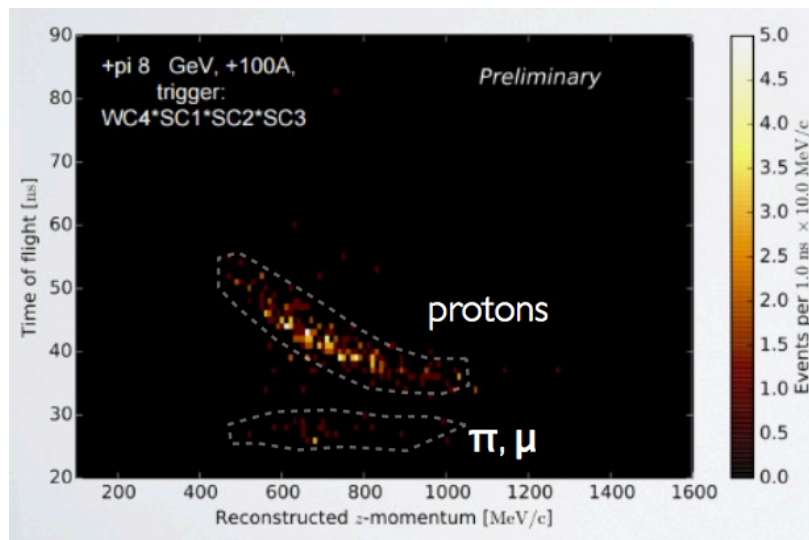


Figure 1 – Time of Flight vs. Reconstructed momentum.

One way we use to discriminate between muon and pions at low momentum is Cherenkov radiation. Cherenkov radiation is a process a charge particle undergoes as it traverses a material faster than the speed of light in that material; it emits light along a cone around the direction of motion. The angle of the cone can be found using a Huygens wavelet construction (see figure).

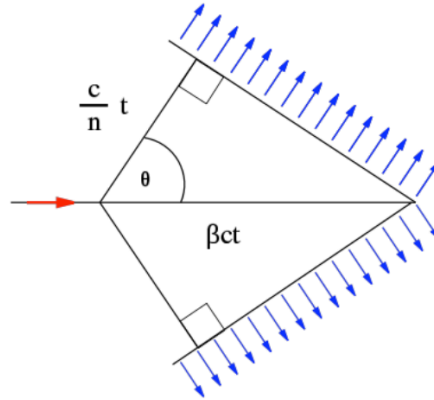


Figure 2 – An overview of the principle of Cherenkov radiation

If n is the index of refraction, the speed of light in the medium is c/n and the angle of emission for a particle of velocity β is $\cos \theta = \frac{1}{\beta n}$. The number of photons emitted per wavelength interval $d\lambda$ per length dx is $\frac{dN_\gamma}{dx d\lambda} = \frac{2\pi Q^2 \alpha}{\lambda^2} \left(1 - \frac{1}{\beta^2 n^2}\right)$. Note that n depends on wavelength and thus the integral over wavelength is finite. Amazingly, the number of photons depends on β and the index of refraction and not on other properties of the medium. The radiated light is biased towards the shorter wavelengths, which is why radioactive materials have a blue glow in water.

Materials and Methods

Aerogel is an ultralight material in which the liquid component of the gel has been replaced with a gas. The result is a solid with extremely low density, low thermal conductivity and low index of refraction.

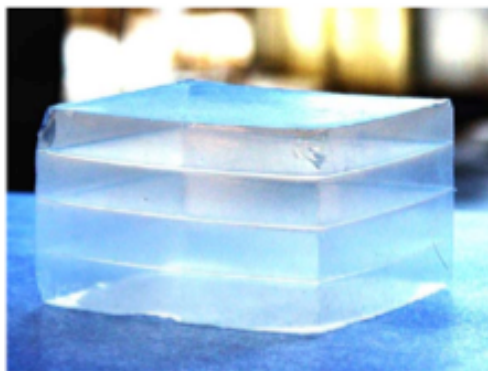


Figure 3 – An picture of Aerogel tiles

Two Photomultiplier tubes (PMTs) and eight tiles of aerogel with an index of refraction of $n=1.05$ were used for the design of the aerogel Cherenkov detector. The design of the aerogel Cherenkov detector optimize to allow the Cherenkov light to travel into the photomultiplier tubes. Having eight tiles aligned horizontal instead of vertical allowed us to increase the thickness for particles to pass through from 6.5 inch to 7.4 inch.

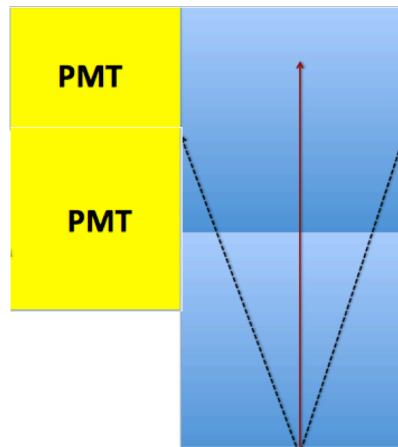


Figure 4 – An overview of the concept of the design of the aerogel Cherenkov detector.

The photomultiplier tubes selected for this design are EMI 9954B 2 inch PMT and XP5382 3 inch PMT. Each photomultiplier tubes was calibrated using LED pulses to select the optimal voltages. This allowed us to translate from analog-to-digital converter (ADC) counts to number of photo- electron (NPEs).

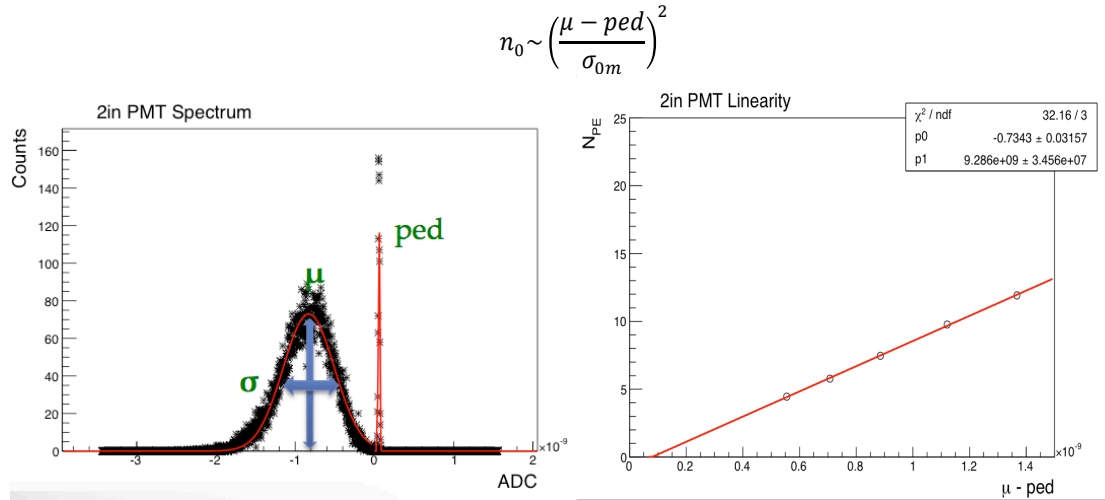


Figure 5-6 – Demonstration of the calibration of a photomultiplier tube.



Figure 7 – XP5382 3 inch photomultiplier tube

After fully constructed and testing, the aerogel Cherenkov detector was placed downstream on the LArIAT Beam line just after another aerogel Cherenkov detector with an index of refraction $n=1.10$, designed and built by our KEK collaborators.

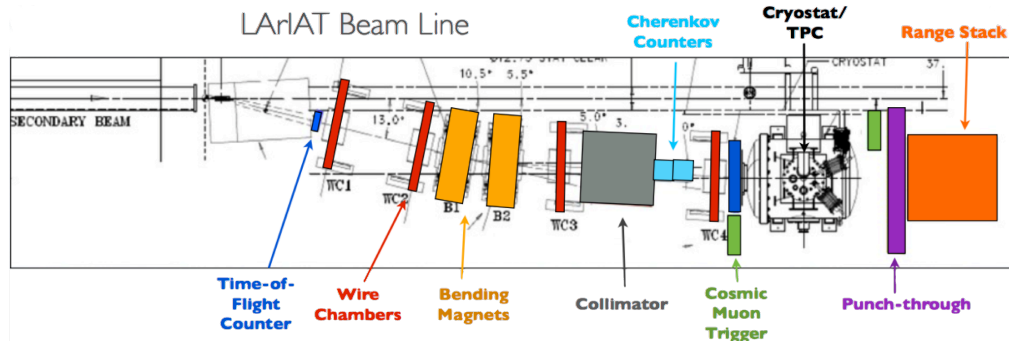


Figure 8 – An overview of LArIAT beam line

The goal of having two aerogel Cherenkov detectors in LArIAT beam line is to separate muons and pions in a momentum range with different index of refraction aerogel, where muons emit Cherenkov radiation while pions do not. The combination of the two aerogel Cherenkov detectors, pions and muons can be identified for momentum less the 400MeV/c.

$$N_{PE} \approx 90 \times \sin^2 \theta_c \text{ where } \cos \theta_c = \frac{1}{\beta n}$$

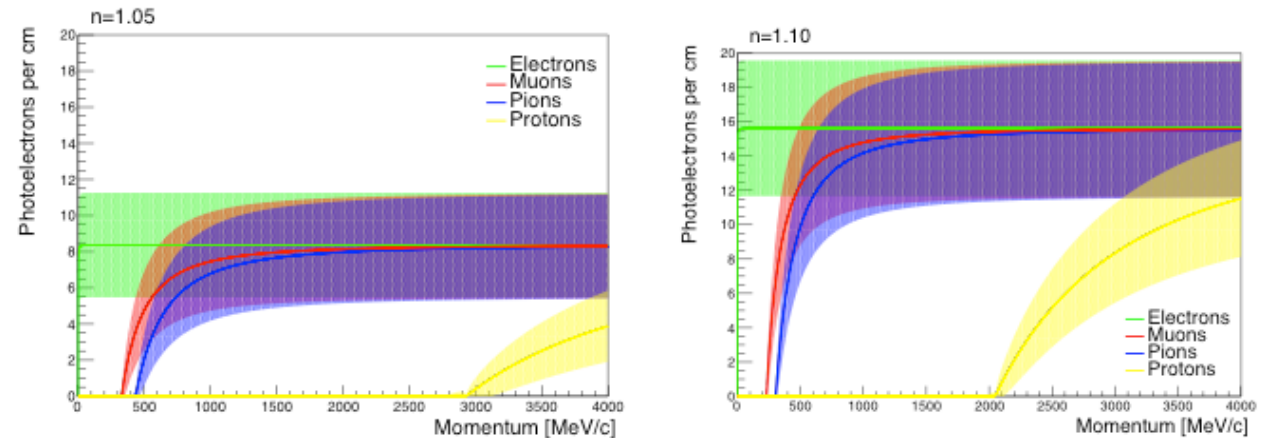


Figure 9-10 – Photoelectrons vs. momentum for both index of refraction of the aerogel.

		n = 1.10	n = 1.05
220<p<285	μ	✓	x
	π	x	x
300<p<400	μ	✓	✓
	π	✓	x

Figure 11 – Table showing where the aerogel Cherenkov detectors would see light and would not.

Results and future work

We were able to extract the time of flight vs. pulse area from both aerogel Cherenkov detectors. Below shows plots of data taking from both negative and positive polarity beam runs. Time of flight selection cuts was made for lower limit of 25ns and upper limit of 48ns. The value to discriminate between pions and protons is 40ns. We will need to get the theoretical calculation to validate the cuts. The threshold for getting the efficiency of detecting specific type of particles

is at 200mV.ns for both pions and protons. Validation can be made after transforming pulse area into number of photoelectrons (NPE).

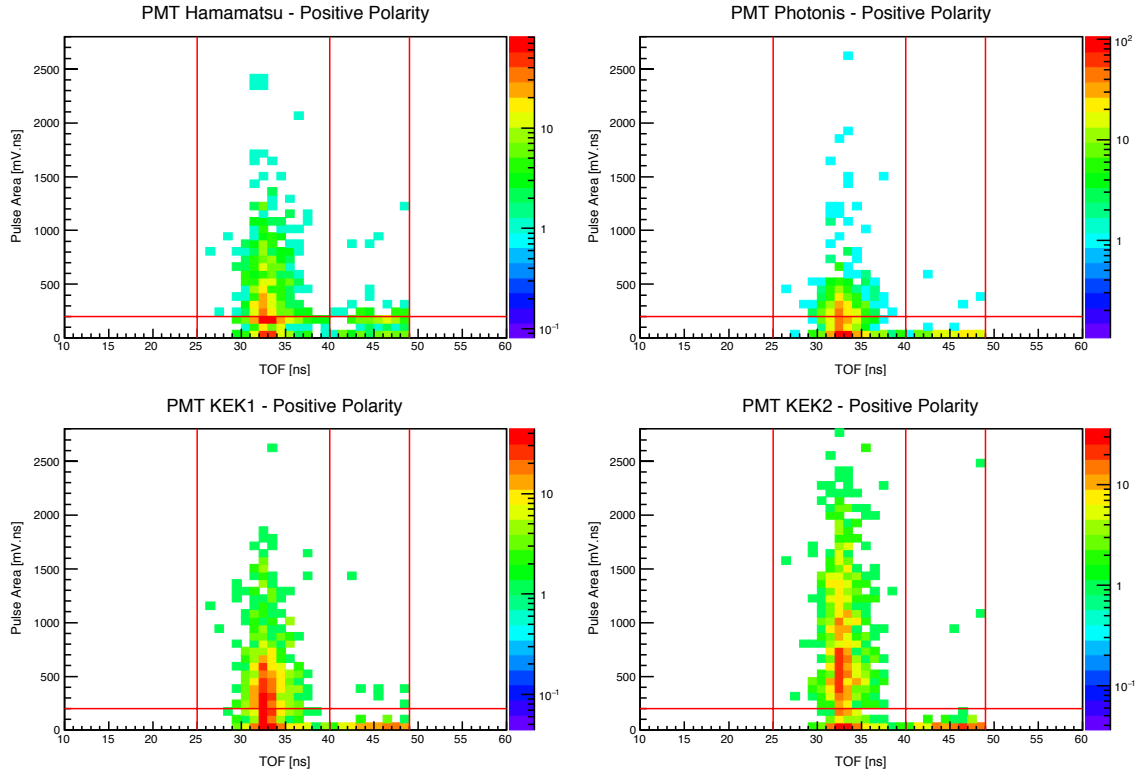


Figure 12 – Plots for TOF vs. Pulse Area – Positive Polarity Runs.

We were able to get the results from the positive polarity magnet beam runs. The efficiency of detecting pions for the Hamamatsu (HMMS) PMT was calculated at 56.70%. The efficiency of detecting pions for the Photonis PMT was calculated at 41.29%. The efficiency of detecting pions for the KEK1 PMT was calculated at 66.63%. The efficiency of detecting pions for the KEK2 PMT was calculated at 81.80%.

The efficiency of detecting protons for the Hamamatsu (HMMS) PMT was calculated at 22.39%. The efficiency of detecting protons for the Photonis PMT was calculated at 29.41%. The efficiency of detecting protons for the KEK1 PMT was calculated at 5%. The efficiency of detecting protons for the KEK2 PMT was calculated at 2.41%.

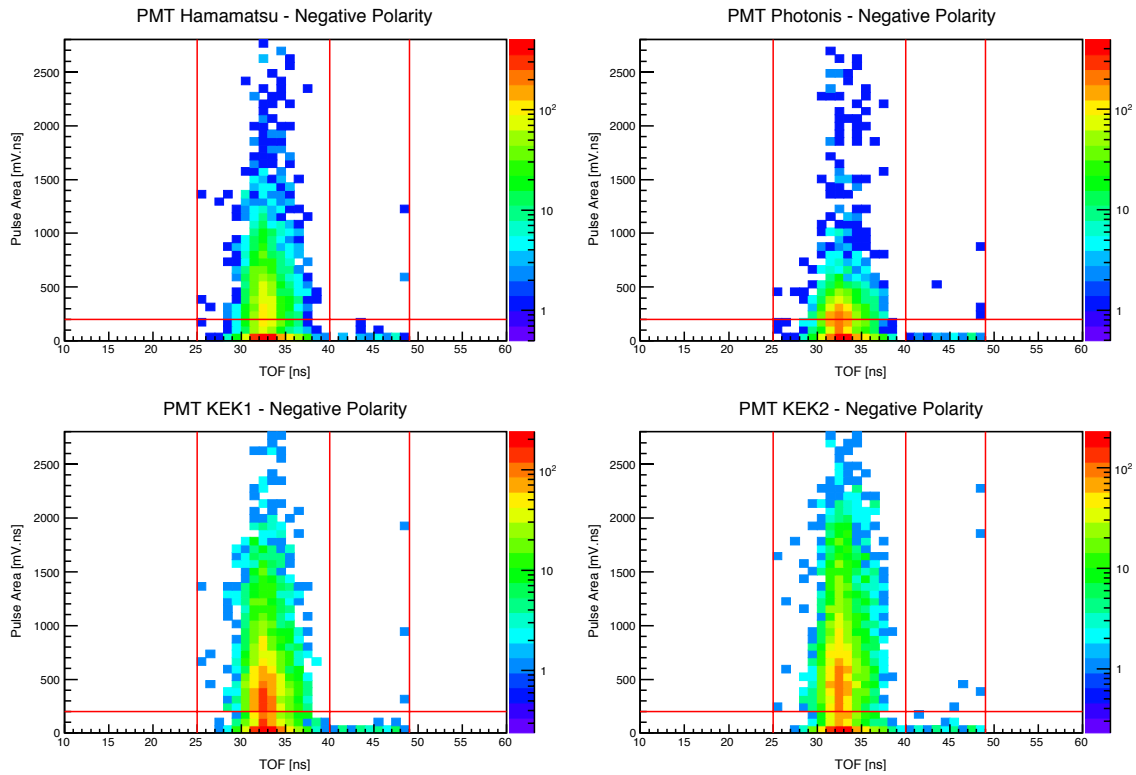


Figure 13 – Plots for TOF vs. Pulse Area – Negative Polarity Runs.

We were also able to get the results from the positive polarity magnet beam runs. The efficiency of detecting pions for the Hamamatsu (HMMS) PMT was calculated at 52.31%. The efficiency of detecting pions for the Photonis PMT was calculated at 41.95%. The efficiency of detecting pions for the KEK1 PMT was calculated at 69.29%. The efficiency of detecting pions for the KEK2 PMT was calculated at 73.98%.

The efficiency of detecting protons for the Hamamatsu (HMMS) PMT was calculated at 10.34%. The efficiency of detecting protons for the Photonis PMT was calculated at 13.79%. The efficiency of detecting protons for the KEK1 PMT was calculated at 8.82%. The efficiency of detecting protons for the KEK2 PMT was calculated at 14.71%.

Acknowledgements

I would like to acknowledge SIST committee for the opportunity to work at Fermilab this summer. I would also like to thank my supervisor and mentors, Jennifer Raaf, Karol Lang, and Will Flanagan for their patience and guidance in my studies for the summer and assistance in the final touches to my paper and presentation and Dũng Phan for his help with the aerogel time of flight vs. pulse area plots.